

CHAPTER 5

MICROBIAL CHROMIUM (VI) REDUCTION IN AQUIFER MEDIA

5.1 Microcosm Study Conceptual Basis

Microbial barrier studies were conducted to simulate the movement of the pollutant across the soil strata into the open aquifer system below the contaminated site. The study takes into consideration the difference in pore structure and organic substrate content in the two layers. The top layer (vadose zone) is characterised by low pore volume and high content of organics from decaying roots and vegetation. The movement of water in the vadose zone is facilitated by weight displacement. If no water enters the vadose zone from above, water will enter this zone from below through capillary action. On the other hand, the aquifer zone has higher pore volume and the water flows under the influence of the hydraulic gradient. The two layers are illustrated in Figure 5-1.

Microcosm samples were collected for the vadose and aquifer microcosm studies at the depths of 1 m and 3 m, respectively. The microcosms were installed in the laboratory as packed-column continuous flow bioreactor systems as described below. Performance of each microcosm was evaluated by comparing the influent and effluent Cr(VI) concentration under sustained hydraulic loading. The shift in microbial community was also monitored by withdrawing soil samples at intervals and analysing the 16S rRNA and 16S rDNA gene sequence for the microbial culture. This was done to determine the presence or absence of Cr(VI) reducers previously identified in the inoculum sludge culture.

The performance of the culture in aquifer media was validated through an *in situ* mesocosm barrier study. The same inoculum culture was used in the barrier system for a laboratory scale mesocosm. Performance in the mesocosm study was evaluated in three dimensional space (along the length, width and depth of the mesocosm). In the following sections, comprehensive results are presented and discussed and a *dispersion-reaction* model is used to determine kinetic and dynamic parameters for the microbial barrier system.

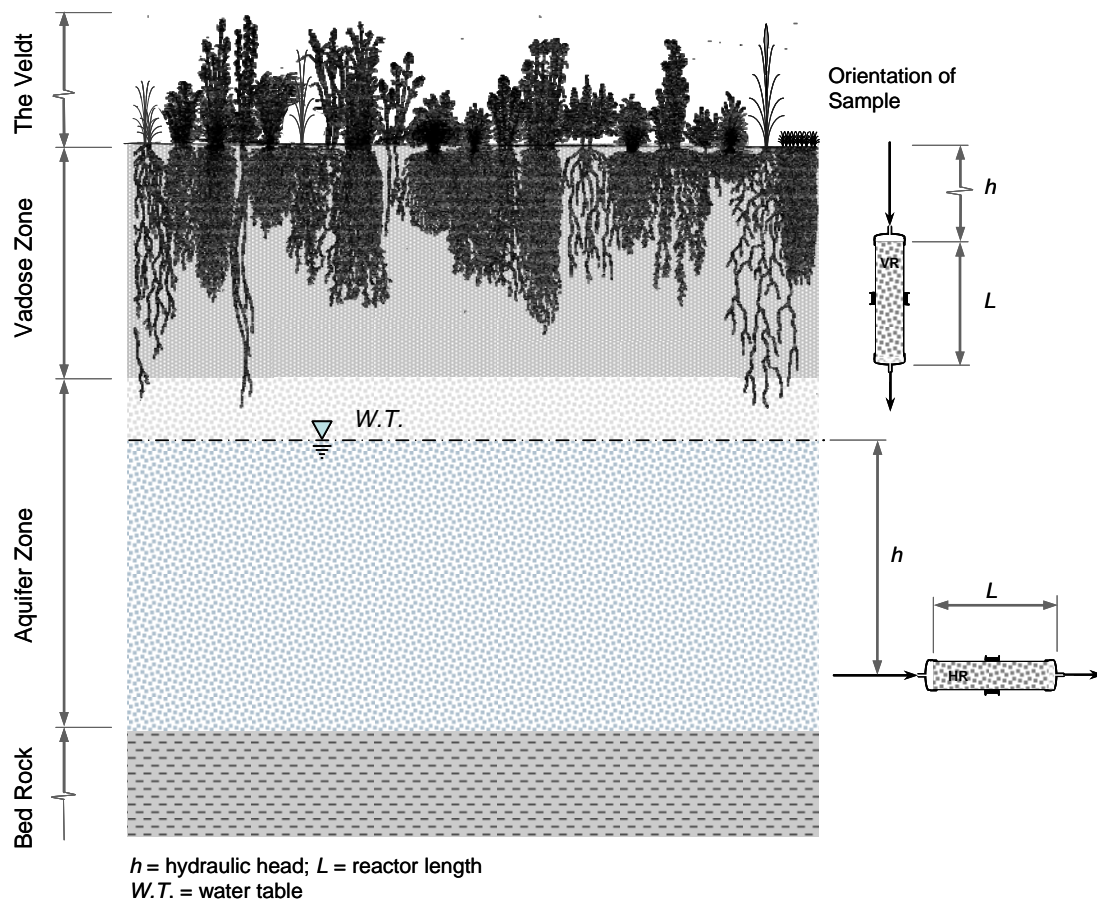


Figure 5-1: Conceptual basis of the microcosm reactor study with vadose media and aquifer media hydraulic effects.

5.2 Performance of Vadose System Microcosm

5.2.1 Cr(VI) Removal Efficiency

These results were obtained for a six-column study (VR1-VR6) using the vadose zone media. All columns were operated under the same hydraulic head. Flow characteristics varied mainly due to slight differences in packing. The operation of Reactors 4 and 5 was discontinued as they experienced severe short circuiting.

From the compiled time series data for the four reactors, it is shown that the reactor inoculated with Cr(VI) reducing bacteria (VR6) achieved near complete removal of Cr(VI) after operation for 16.7 days under a slow feed (flow rate, $Q = 0.310 \text{ cm}^3/\text{hr}$). Up to 95% Cr(VI) removal was observed in this reactor. However, operation of VR3 at almost twice the flow rate of VR6 resulted in decreased efficiency in the Cr(VI) reduction process. The removal rate in VR3, which was also inoculated with live sludge bacteria, but operated at a high flow rate of $0.608 \text{ cm}^3/\text{h}$, was approximately 80%, much lower than the Cr(VI) removal rate in VR6. The time series data for the four reactors including the control are shown in Figure 5-2. No Cr (VI) removal was observed in the sterilised, non-inoculated control (VR2). The operation conditions and final performance of the reactors is summarized in Table 5-1.

Table 5-1: Performance of gravity-fed vadose microcosm reactors operated under an influent Cr(VI) concentration of 40 mg/L.

Reactor (Column No.)	Flow Rate cm^3/h	Effluent Cr(VI) mg/L	Effluent Cr(III) mg/L	Cr(VI) Removal %
Native-soil (VR1)	0.614	39.0 ± 2.0	0.0 ± 0.0	0.0 ± 0.0
Non inoculated (VR2)	0.310	37.8 ± 1.5	0.0 ± 0.0	0.0 ± 0.0
Inoculated (VR3)	0.608	6.7 ± 0.8	1.5 ± 0.4	80 ± 3.6
Inoculated (VR6)	0.310	1.9 ± 0.3	3.2 ± 1.1	95.3 ± 1.4

In the sterile reactor (VR2), effluent Cr(VI) concentration increased to the influent level and remained there until the experiment was concluded after 400 hours (16.7 days). The two data points at 84 and 96 hours showed removal up to 49% (Figure 5-2), but this was later attributed to system error on the spectrometric measurement. Based on this data, a theoretical hydraulic retention time (HRT) was estimated at 8.67 hours for the control reactor which was later used in a tracer analysis.

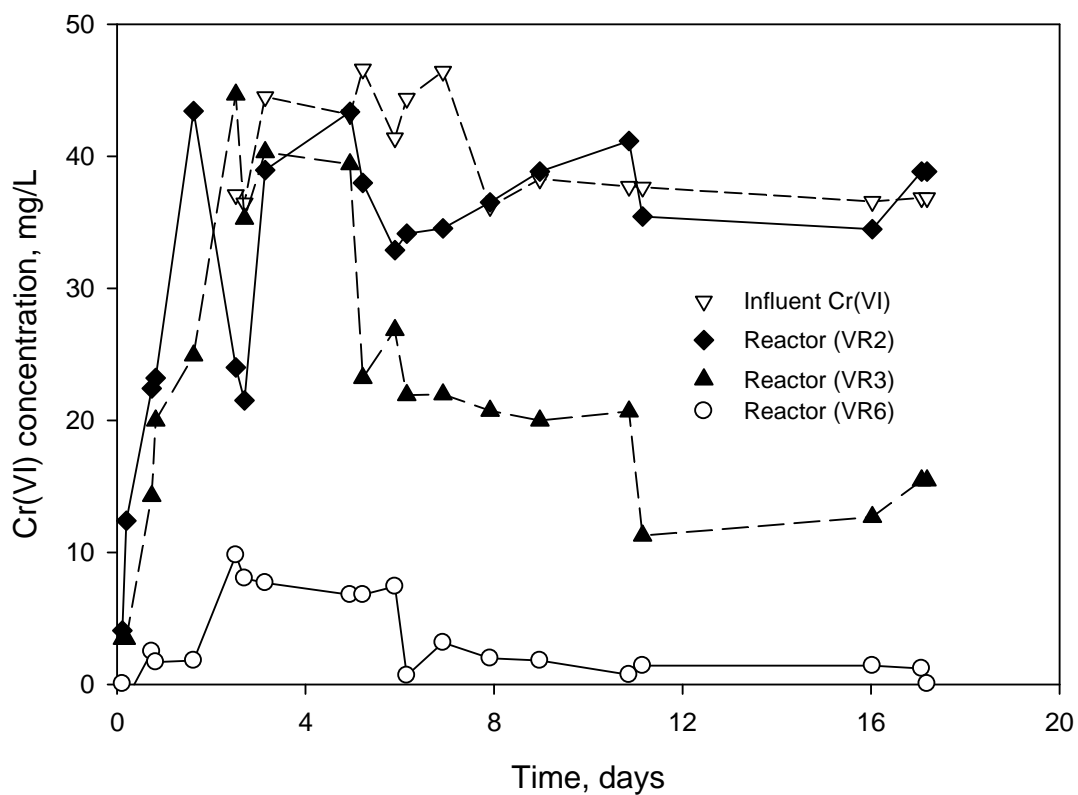


Figure 5-2: Influent and effluent Cr(VI) data in vadose reactors VR2 – sterilised column; VR3 – inoculated non-sterile reactor at $0.608 \text{ cm}^3/\text{h}$; and VR6 – inoculated non-sterile reactor at $0.310 \text{ cm}^3/\text{h}$.

5.2.2 Cr(VI) Speciation in the Vadose Microcosm Reactors

Studies in batch systems showed that Cr(VI) was reduced to Cr(III) using the dried sludge consortium cultures. In the batch studies, all Cr(VI) reduced was accounted for

as Cr(III) (Molokwane *et al.*, 2008). Cr(III) is known to readily precipitate as chromium hydroxide ($\text{Cr}(\text{OH})_3(\text{aq})$) at pH above 6.5 (Morel and Herring, 1986).

In this study, measurement of total Cr in the effluent from the inoculated microcosms correlated with the measurements of Cr(VI) in the effluent suggesting that most of the Cr(III) produced was trapped in the columns as amorphous $\text{Cr}(\text{OH})_3(\text{aq})$ (Table 5-1). Longer-term studies showed a characteristic decrease in flow indicating reduction of pore space for the free flow of water due to continuous Cr(III) precipitation. Additionally, a characteristic change in colour – to dark-green – was observed in the reactors with high Cr(VI) reduction (VR3 and VR6) showing accumulation of Cr(III) in the pores of the aquifer media. The other factor that contributed to decrease in flow is the growth of bacteria most of which remained trapped in the reactors.

5.2.3 Microbial (culture) dynamics in Vadose Systems

Characteristics of Initial Consortium

The dry sludge culture used to inoculate the vadose zone reactors was grown under aerobic to microaerobic conditions. The operation of the area for 15 days was determined to be not long enough to completely eliminate facultative bacteria in the reactors. This was evidenced by the presence of significant amounts of *Bacillus* species from the original inoculum. Partial sequences of 16S rRNA matched the *Bacillus* groups – *Bacillus cereus* ATCC 10987, *Bacillus cereus* 213 16S, *Bacillus thuringiensis* (serovar finitimus), *Bacillus mycoides* – and two *Microbacterium* species – *Microbacterium foliorum* and *Microbacterium* sp. S15-M4. A phylogenetic tree was constructed for the species from purified cultures grown under aerobic conditions based on results from a basic BLAST search of rRNA sequences in the NCBI database (Figure 5-3a).

Characterisation of Microcosm Bacteria (After 15 days)

After operating the reactors under oxygen stressed conditions in the presence of other soil bacteria, a community shift was expected. In reactors VR3 and VR6, the soil contained a wide range of soil dwelling species of bacteria as well as the newly introduced bacteria from the dried sludge. The microbial dynamics monitored by the 16S rRNA fingerprinting showed a decrease in culturable species after exposure to Cr(VI) as shown in Tables 5-2. Only the *Bacillus cereus* and *Bacillus thuringiensis* serotypes persisted either due to resilience against toxicity or adaptation to the changing conditions in the reactor. The *Lysinibacillus* group is also a well known sludge bacteria. Both *Bacilli* (*Bacillus cereus* and *Bacillus thuringiensis*) and the *Lysinibacillus* species contain well known Cr(VI) reducing serotypes such as *Bacillus* K1 (Shen *et al.*, 1996), *Bacillus cereus*, *Bacillus thuringiensis* (Francisco *et al.*, 2002; Camargo *et al.*, 2003; Faisal and Hasnain, 2006), and *Lysinibacillus sphaericus* AND 303 (Pal *et al.*, 2005).

The microbial community shift is indicated by the appearance of the *Lysinibacillus* *sp.* and *B. drentensis* which were not detectable in the original soil and sludge cultures (Table 5-2). The *B. drentensis* and *L. sphaericus* probably originated from the sludge used for inoculation. Among these two new species, *L. sphaericus* is known to produce a Cr(VI) reductase – an enzyme responsible for Cr(VI) reduction utilising a mechanism independent from the membrane respiratory pathway (Pal *et al.*, 2005). When cultured under anaerobic conditions, more Gram-negative species emerged that were not observed under aerobic and microaerobic conditions.

Performance of Native Species

Cr(VI) reduction by native species in soil acting alone was insignificant. The predominant species from the soil include *Rhizobium spp.*, *Pseudomonas spp.*, and

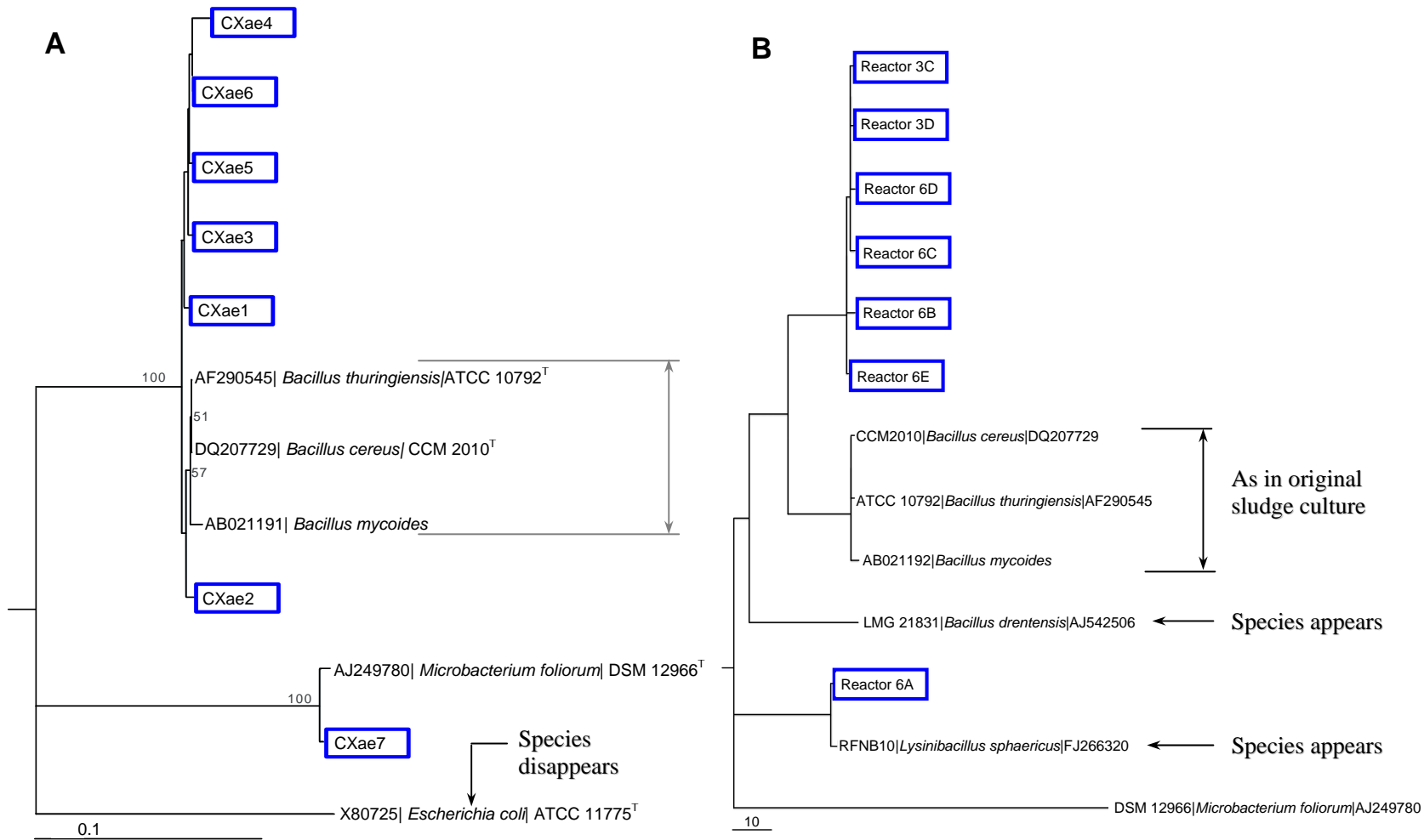


Figure 5-3: Comparative culture analysis at day 1 (a) and day 15 (b) in the vadose media microcosm experiment showing the disappearance of *Escherichia coli* and appearance of *Bacillus drentensis* and *Lysinibacillus sphaericus* at the end of the experiment.

Klebsiellae and many others. Most of the bacteria from the soil could not be cultured. However, the cultures detected are the ones that were resistant to Cr(VI). No significant Cr(VI) reduction was observed in the reactor that contained only bacteria from the soil (VR1). The performance did not improve after long term exposure and reloading the reactor with the 40 mg/L feed.

Table 5-2: Summary of microbial culture changes after operation of the microcosms reactors for 15 days under an influent Cr(VI) concentration of 40 mg/L.

Inoculation culture Consortium		Culture in Reactor 3 and 6 at end of experiment	
Type	Predominant species	Type	Predominant species
X1	<i>Bacillus cereus</i> 213 16S, <i>Bacillus thuringiensis</i> 16S	A	<i>Pantoea</i> or <i>Enterobacter</i> sp.
X2	<i>Bacillus cereus</i> ATCC 10987, <i>Bacillus thuringiensis</i> str. Al Hakam	B	<i>Bacillus</i> sp. possibly <i>Bacillus thuringiensis</i> / <i>cereus</i> group
X3	<i>Bacillus cereus</i> ATCC 10987, <i>Bacillus thuringiensis</i> str. Al Hakam	C	<i>Pantoea</i> or <i>Enterobacter</i> sp.
X4	<i>Bacillus mycoides</i> BGSC 6A13 16S. <i>Bacillus thuringiensis</i> serovar <i>finitimus</i> BGSC 4B2 16S	D	<i>Lysinibacillus sphaericus</i> strain BG-B111, <i>Bacillus</i> sp. G1DM-64, <i>Bacillus sphaericus</i>
X5	<i>Bacillus mycoides</i> BGSC 6A13 16S. <i>Bacillus thuringiensis</i> serovar <i>finitimus</i> BGSC 4B2 16S	E	<i>Bacillus</i> sp. possibly <i>Bacillus thuringiensis</i> / <i>cereus</i> group
X6	<i>Bacillus mycoides</i> BGSC 6A13 16S. <i>Bacillus thuringiensis</i> serovar <i>finitimus</i> BGSC 4B2 16S	F	<i>Bacillus</i> sp. possibly <i>Bacillus thuringiensis</i> / <i>cereus</i> group
X7	<i>Bacillus mycoide</i> BGSC 6A13 16S. <i>Bacillus thuringiensis</i> serovar <i>finitimus</i> BGSC 4B2 16S	G	<i>Bacillus cereus</i> strain ZB

5.3 Performance of the Main Aquifer Microcosm

Soil columns extracted from the aquifer (below the water table) were installed in a continuous dose experiment as shown in Figure 5-4. Eight microcosm columns were installed with the first acting as the control, Reactor HR2 evaluates the sludge bacteria acting alone, and Reactors HR3 and HR4 evaluate the native soil bacteria acting alone (in duplicate). The main experiments comprised (in duplicate) HR5 and HR6 with both sludge bacteria and native soil bacteria but operated without carbon source, and HR7 and HR8 with soil bacteria and sludge bacteria operated with added carbon source. The carbon source in HR7 and HR8 consisted of a natural matrix of organics leached from saw dust. This was intended to simulate humic organics leaching from stems of dead plants in the Veldt. The experimental plan for the detailed evaluation of the performance of aquifer microcosm reactors is summarised in Table 5-3.

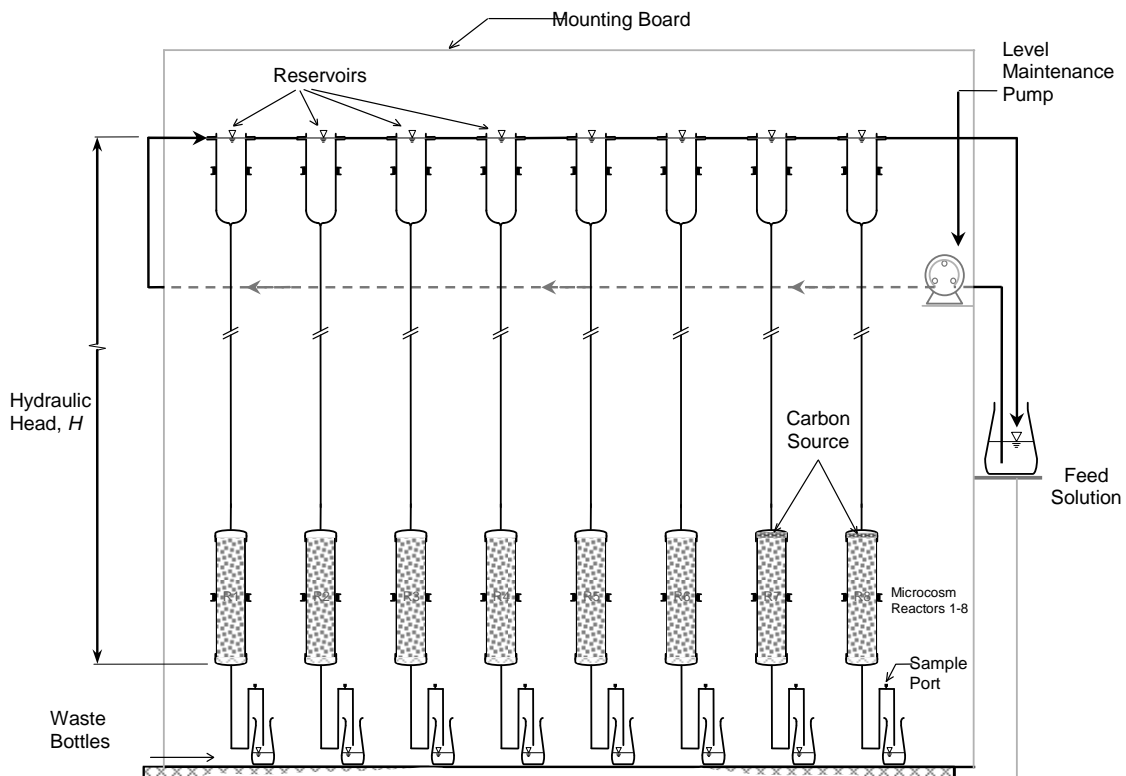


Figure 5-4: Main aquifer microcosm columns (HR1-HR8) to simulate the performance of microbial barrier systems in aquifer media.

Table 5-3: Conditions for the aquifer microcosm range of experiments.

Reactor(s)	Experiment
Reactor HR1	Sterilised (killed native bacteria) + no inoculation
Reactor HR2	Sterilised (killed native bacteria) + inoculated (sludge bacteria)
Reactors HR3 and HR4	Live native soil bacteria (non-sterile) + no inoculation
Reactors HR5 and HR6	Live native soil bacteria (non-sterile) + inoculated (sludge bacteria)
Reactors HR7 and HR8	Live native soil bacteria (non-sterile) +inoculated + carbon source

5.3.1 Evaluation of the Abiotic Process in the Microcosms

The operation of the sterilised reactor without added biomass showed a characteristic rise following the effluent tracer line for the clean-bed reactor system (Figure 5-5). The characteristic exponential rise suggests that adsorption processes were insignificant, i.e., the column reached equilibrium with respect to adsorption during the 45 days of operation. The extended controls Reactors HR2, HR3 and HR4 show that soil bacteria and activated sludge bacteria acting alone in these conditions did not reduce Cr(VI). The reason why the soil bacteria could not reduce Cr(VI) is most certainly because there were no Cr(VI) reducing bacterial species in the soil. However, it is not known why the sludge bacteria did not reduce Cr(VI) after inoculating a sterile column. One suggestion is that the Cr(VI) bacteria from the sludge required some biochemical metabolites or cofactors produced by the soil bacteria.

5.3.2 Cr(VI) Reduction by Inoculated Natural Soil without Carbon Source

The first indication of significant Cr(VI) reduction was observed in the reactors containing live cultures of both soil bacteria and dried sludge bacteria (Reactors HR5 and HR6) (Figure 5-6). The operation of Reactor HR6 was later discontinued due to

severe short circuiting. Cr(VI) reduction in the reactors HR5 and HR6 was achieved in absence of any carbon source. It is suggested that Cr(VI) reducing bacteria from the sludge required certain cofactors or metabolites from the native bacteria in the soil. Up to 66% Cr(VI) removal was achieved by the mixed culture growing without a carbon source (Figure 5-6). The bacteria in these reactors were expected to be predominantly anaerobic due to the longer period of operation in the absence of oxygen. It was therefore expected that some of the bacteria could utilise inorganic carbon sources such as bicarbonate (HCO_3^-) for cell synthesis and sulphides and nitrates in the soil as electron donors and energy sources.

5.3.3 Cr(VI) Reduction by Inoculated Natural Soil with added Carbon Source

The best performance was observed in reactors with live native soil bacteria (non-sterile soil column) inoculated with sludge bacteria in the presence of the carbon source (saw dust) (Reactors HR7 and HR8, Figure 5-7). Cr(VI) removal under a lower hydraulic loading of $304 \text{ cm}^3/\text{d}$ was 93% after 45 days. The Cr(VI) removal under a higher hydraulic loading of $433 \text{ cm}^3/\text{d}$ was 78%. These results show that the Cr(VI) reducing culture derived more energy from an organic carbon source than from the inorganic sources. This finding is consistent with previous conclusions by other researchers where it was determined that Cr(VI) reduction is an energy intensive process drawing energy resources from the cellular housekeeping processes (Chirwa and Wang, 2000; Ishibash *et al.*, 1990).

5.3.4 Cumulative Cr(VI) Reduction in the Microcosm Systems

From the determination of cumulative Cr(VI) reduction in the microcosms over time (Figure 5-8), it was shown that the highest Cr(VI) reduction rate ($5.69 \text{ g Cr(VI)}/\text{m}^3/\text{d}$); was achieved in the Reactor HR7 operated under a low hydraulic loading $0.403 \text{ cm}^3/\text{d}$ with carbon sources introduced through a layer of saw dust and reactor HR8 at a

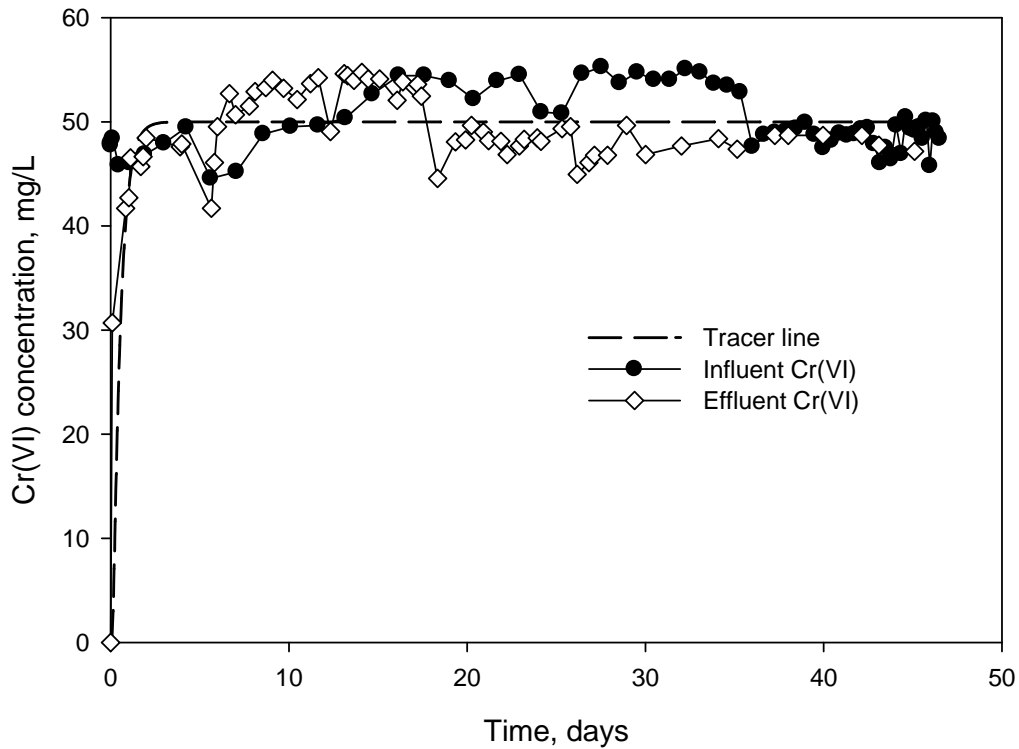


Figure 5-5: Performance of a non-inoculated sterile column showing a characteristic exponential rise in effluent Cr(VI) comparable to the tracer.

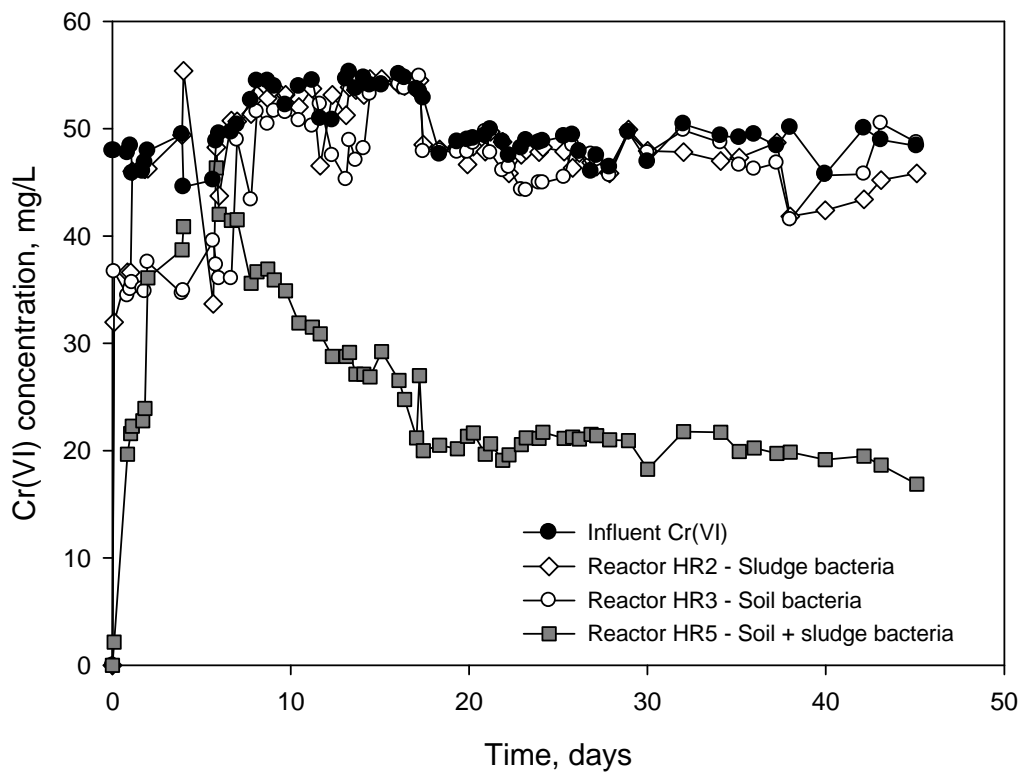


Figure 5-6: Performance comparison: sludge culture acting alone (HR2), soil culture acting alone (HR3), and the combination of sludge and soil bacteria (HR5).

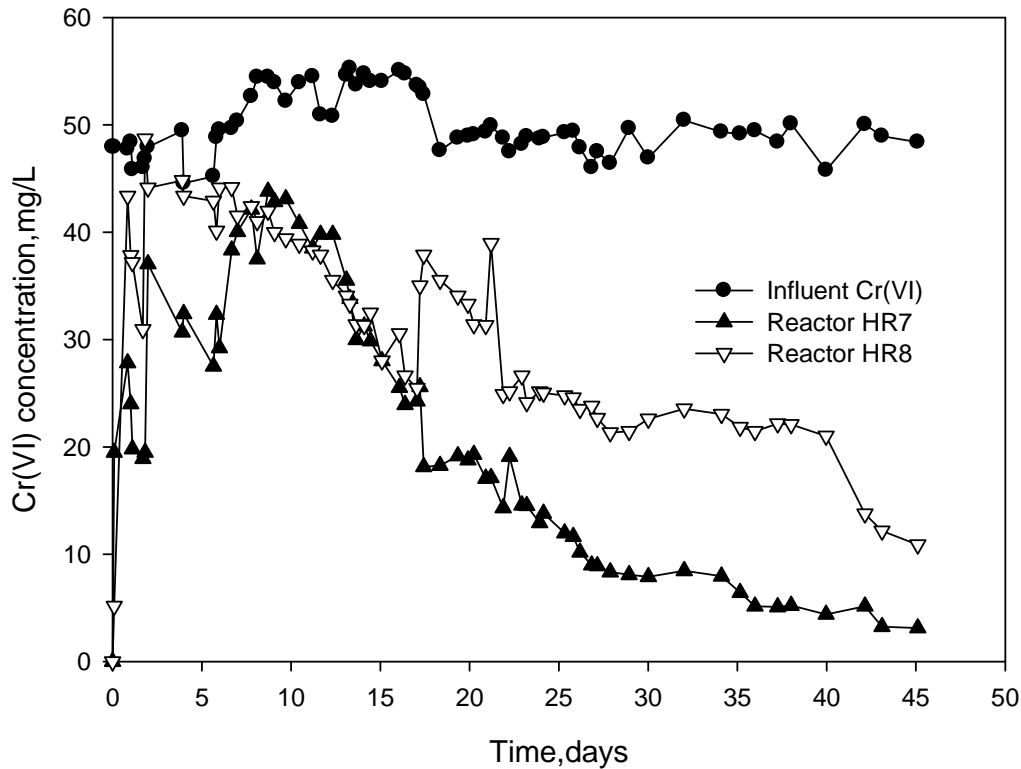


Figure 5-7: Performance of the reactors containing live cultures of sludge bacteria and native soil species (Reactors HR7 and HR8) operated with carbon sources leached from saw dust.

slightly higher hydraulic loading $0.433 \text{ cm}^3/\text{d}$ with carbon sources introduced by the presence of saw dust ($4.54 \text{ g Cr(VI)}/\text{m}^3/\text{d}$) (Figure 5-8). The reactor with no carbon source but with both sludge and soil bacteria in the starter culture (Reactor HR5) achieved the next highest performance ($3.08 \text{ g Cr(VI)}/\text{m}^3/\text{d}$). The reactors HR5, HR7 and HR8 did not reach their Cr(VI) reduction capacity as demonstrated by the continuing increase in the cumulative Cr(VI) removal slope. It is however expected that at one point, Cr(VI) reduction capacity could be lost mainly due to blocking of pores with Cr(III) precipitate.

Insignificant cumulative Cr(VI) removal was observed in the sterile reactor control (HR1) and the reactors with soil bacteria and sludge bacteria acting alone HR3 (Figure 5-8).

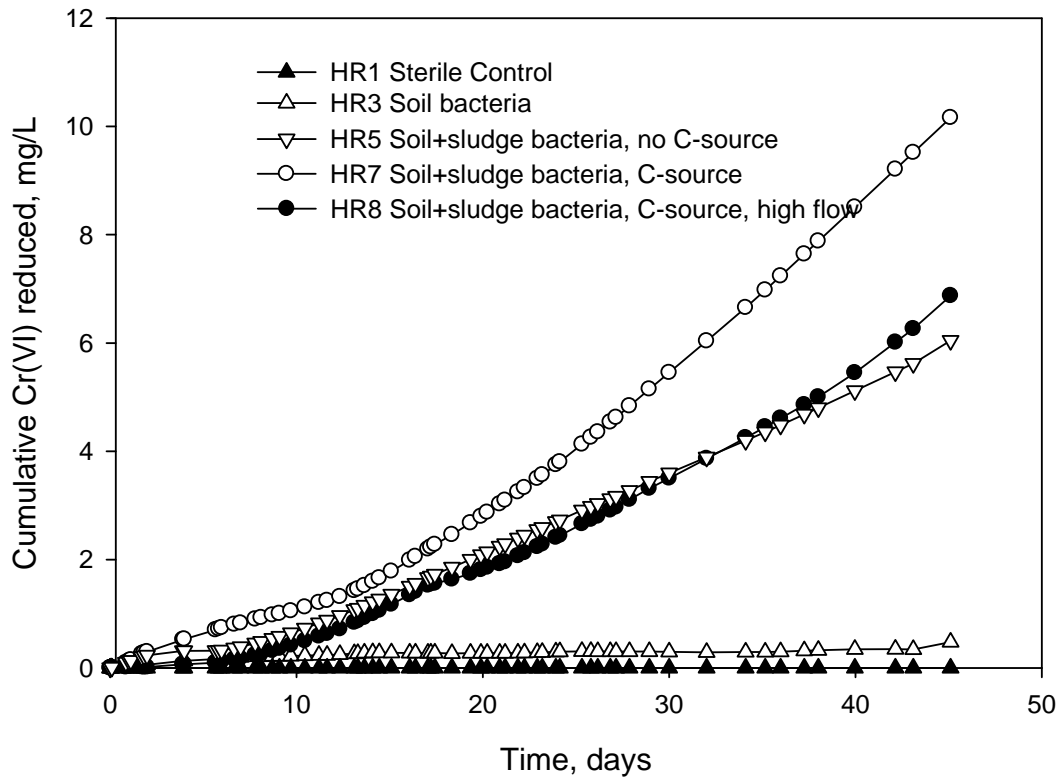


Figure 5-8: Cumulative Cr(VI) removal in the aquifer microcosm reactors showing that the reactors had not reached their full capacity.

5.3.5 Performance Summary

Overall performance of different reactors is summarised in Table 5-4. The results show that the presence of the carbon source had a significant impact on the Cr(VI) reduction rate in the microcosms. Up to 93% removal is achieved in HR7 with carbon source after operation for 45 days. Reactor HR5 without carbon source achieved approximately 66%. The high performance in reactors with live bacteria from both the soil and sludge is demonstrated by the maximum Cr(VI) removal rates (Table 5-4, last column).

Table 5-4: Capability of mixed cultures in reducing Cr(VI) in aquifer microcosms at day 45.

Reactor No.	Flow rate (Q) cm ³ /h	Measured Cr(VI) (Effluent) mg/L	Total Removal % (at day 45)	Removal Rate g Cr(VI)/m ³ /d
HR1	0.660	47.2	0	0
HR2	0.259	45.8	4.5	0.07
HR3	0.714	48.7	0	0.37
HR4	0.290	48.8	0	0.56
HR5	0.228	16.9	66.3	3.08
HR6	0.430	13.5	73.0	--
HR7	0.304	3.1	93.0	5.69
HR8	0.433	10.9	78.2	4.54

5.4 Microbial Culture Dynamics in Aquifer Media Microcosm Reactor

5.4.1 Analysis under Anaerobic Conditions

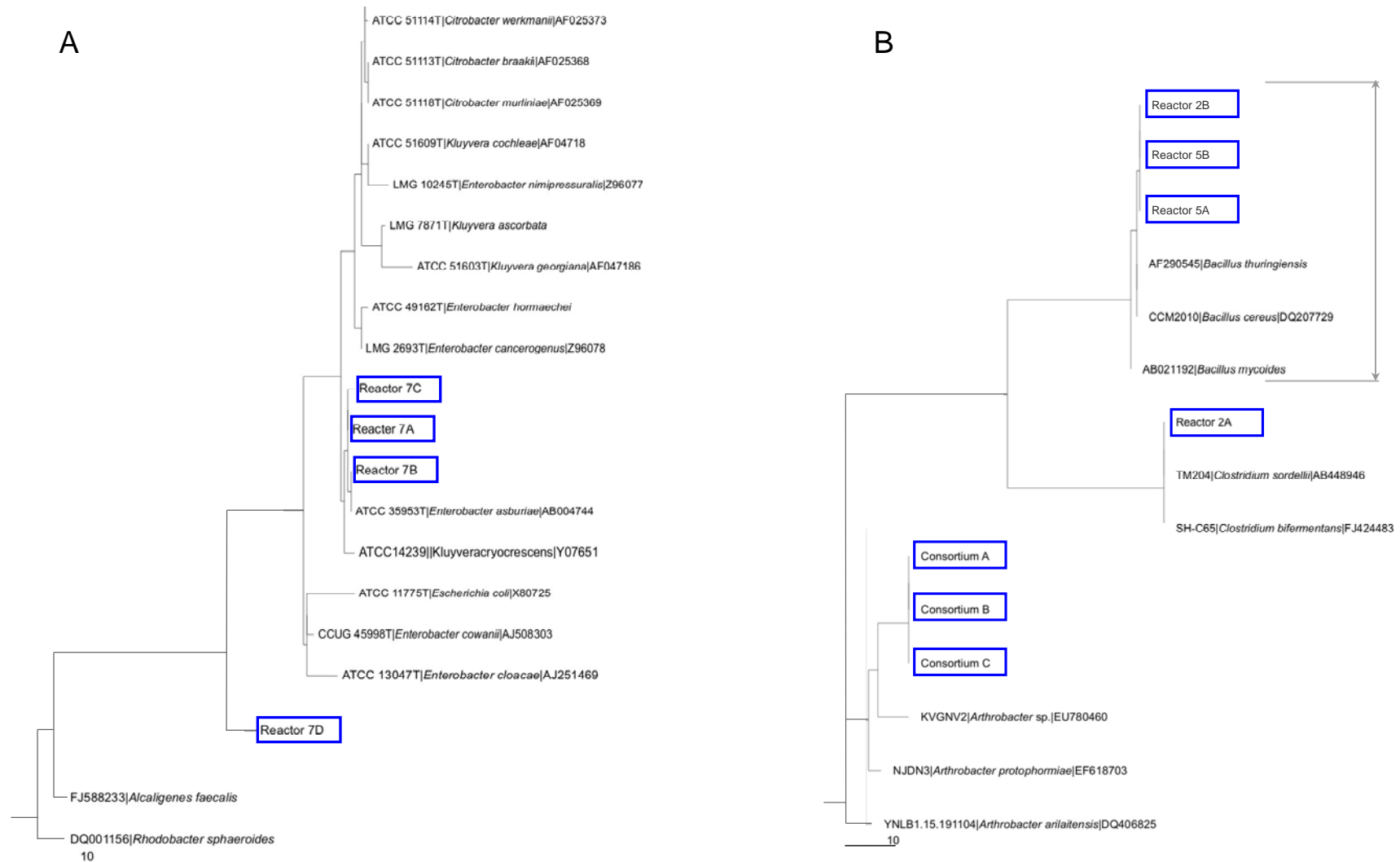
Due to the oxygen deprivation conditions of the deeper microcosm and operation for a longer period, consideration was given for the anaerobic microbial composition of the start-up culture. Both the sludge bacteria and soil bacteria favouring anaerobic conditions were analysed and the results obtained were presented in phylogenetic tree diagrams (shown in Appendix 2).

The results showed the predominance of *Microbacterium*, *Acinetobacter*, *Arthrobacter*, *Brevibacterium*, *Rumen bacteria*, and several *Enterococci* in the sludge culture and *Arthrobacter spp.*, *Clostridium spp.*, and *Klebsella spp.* and several unidentified unculturable species in the soil cultures. None of the identified soil bacteria were recognised from literature as Cr(VI) reducing species. However, several species from the sludge culture tested positive in their capability to catalyse the reduction of Cr(VI) to Cr(III).

5.4.2 Characteristics of Microorganisms in the Microcosm after 45 days

The cultures were analysed again after 45 days to determine the microbial shift and microorganisms responsible for the observed Cr(VI) reduction especially in the Reactors HR5, HR7 and HR8. The results were once again presented in phylogenetic tree diagrams for ease of comparison between the different cultures under the different Cr(VI) exposure conditions (Figure 5-9). The results showed a wider biodiversity in the gram-negative species. Most of the G-negative species are predicted to be anaerobic thus are capable of growing on a variety of carbon sources including inorganic carbon sources. The long-term operation conditions in the aquifer microcosm experiments favoured these species.

Cr(VI) reduction in anaerobic cultures of bacteria was previously determined to be slower than the reduction in aerobic cultures (Shen and Wang, 1993). This is attributed to the faster metabolic rate in the aerobic cultures. The Cr(VI) removal in the vadose microcosm (VR) systems was much faster than in the deeper microcosm (HR) systems. The slower Cr(VI) removal rate in the aquifer microcosms (HR system) was mainly due to the proliferation of obligate anaerobes and higher sensitivity to Cr(VI) toxicity in these organisms.



79 **Figure 5-9:** Analysis of the consortium culture from the microcosms after 45 days: (a) gram-negative species (b) gram-positive species.

5.5 Simulation of Cr(VI) Reduction in Microcosm Systems

5.5.1 Model Description – Advection/Reduction Model

The microcosm reactors were modelled as plug flow reactors with the Cr(VI) removal influenced by the following internal processes: (1) advection influenced by the interparticle velocity u (LT^{-1}), (2) mass transport into media particles governed by mass transport rate coefficient k_L (LT^{-1}), (3) adsorption rate governed by mass transport and surface reaction, (4) Cr(VI) reduction governed by the kinetics described in Chapter 4, and (5) cell replacement rate with the cells acting as the catalyst in the Cr(VI) reduction process. The above fundamental processes in the reactor during transient state operation can be represented by the Equations 5-1 to 5-5 below:

$$\frac{dV}{dt} = u \cdot A \quad (5-1)$$

$$\frac{dC}{dt} = -k_L a (C - C_s) = -j_c \quad (5-2)$$

$$\frac{dC}{dt} = -k_{ad} (C_{eq} - C) = -q_c \quad (5-3)$$

$$\frac{dC}{dt} = -\frac{k_m \cdot C}{K^{1-Cr/C_0} \cdot (K_c + C)} \left(X_0 - \frac{C_0 - C}{R_c} \right) = -r_c \quad (5-4)$$

$$\frac{dX}{dt} = Y \left(\frac{k_{ms} S}{K_s - S} \right) - k_d X \quad (5-5)$$

where C_s = Cr(VI) concentration at the particle surface (ML^{-3}), C_{eq} = equilibrium concentration at the surface for the adsorptive process (ML^{-3}), the coefficient k_L = mass transport rate coefficient (LT^{-1}), a = total surface area in the reactor (L^2), k_{ad} = adsorption rate coefficient (T^{-1}), Y = cell yield coefficient ($M \cdot M^{-1}$), k_{ms} = specific

substrate utilisation rate coefficient (T^{-1}) and k_d = cell death rate coefficient (T^{-1}). The interstitial space A in the microcosm was estimated as the volume of the mobile phase (bulk liquid) minus entrained water determined as the difference between the weight of the wet non-flowing reactor and a dry reactor. The process terms: j_c = mass transport rate ($ML^{-2}T^{-1}$), q_c = adsorption rate ($ML^{-3}T^{-1}$), and r_c = Cr(VI) reduction rate ($ML^{-3}T^{-1}$). Since the aquifer reactors were operated under predominantly anaerobic conditions, Cr(VI) reduction with toxicity threshold inhibition (Equation 4-15) was chosen during the simulation. Equation 4-15 is rearranged for the AQUASIM format as shown in Equation 5-4. The reaction rate and inhibition coefficients as determined from batch experiments were maintained in the continuous flow systems with minor adjustments permitted due to different culture sensitivity as the microbial community shifted to more gram-negative anaerobic species.

Due to space limitations in the reactor, cells could only grow to a certain maximum concentration. The time at which the cells reached the maximum allowable concentration was dependent on initial cells, Cr(VI) toxicity and hydraulic loading rate. These conditions caused the cells to obey a logistic function as shown in Equation 5-6 below:

$$X = X_0 + \frac{X_{\max}}{1 + \left(\frac{t}{t_0}\right)^b} \quad (5-6)$$

where X = viable cell concentration (ML^{-3}) at any time t (T), X_{\max} = maximum attainable viable cell concentration (ML^{-3}) in the microcosm, t_0 = logistic interval (T), and b = pitch (dimensionless). The impact of the adsorptive process was determined to be minimal based on an earlier tracer study (Figure 5-5). In the adsorptive process, equilibrium was reached within hours of operation, but the experiment was extended

to 45 days. The predominant processes in the reactor are thus limited to advection, reduction, mass transport and cell growth. These processes were used in the mass balance for Cr(VI) removal across the bulk liquid phase in the microcosm reactor:

$$\frac{d(C \cdot V)}{dt} = A \sum_{l=0}^{l=L_i} u(C_{in} - C) + j_c \cdot a_i + (q_c + r_c) \cdot \Delta V \quad (5-7)$$

where, for each segment of reactor of length ΔL (L), ΔV = change in reactor volume (L^3), the interstitial velocity u (LT^{-1}) is assumed to be constant throughout the entire reactor, a_i = surface area in the segment (L^2). The adsorption rate, q_c ($ML^{-3}T^{-1}$) Approaches zero in the order of 6 to 10 hours. The Cr(VI) reduction rate, r_c ($ML^{-3}T^{-1}$), is a function of viable biomass in the reactor. Table 5-5 shows the description of parameters used. Time series data was simulated in the Software for Simulation of Aquatic Systems (AQUASIM 2.0) software shown in Appendix C.

Table 5-5: Definition of parameters used.

Parameter	Description	Value/Units
Q	Flow rate	m^3/d
C_{in}	Influent Cr(VI) concentration	mg/L
C	Cr(VI) concentration (state variable)	mg/L
a	Surface area	m^2
A	Effective cross sectional area	$4.6 \times 10^{-4} m^2$
F	Input Cr(VI), $Q \cdot C_{in}$	mg/d
D	Coefficient of molecular diffusion	$98.4 m^2/d$
ΔL	Grid section	m
N	Grid number	52
C_{eq}	Equilibrium/saturation concentration	mg/L
X_0	Initial viable cell concentration/density in the reactor	$23.5-4.5 g/m^3$
X_{max}	Maximum attainable viable cell concentration	$3.5-65.3 g/m^3$
t_0	Logistic interval for biomass	10.4-20.4 d
b	Logistic pitch for the biomass	dimensionless
t	Time (programme variable)	d

5.5.2 Simulation of Control Conditions

The performance of the reactor in the absence of viable biomass X is shown previously in Figure 5-5. Application of the mass balance model (Equation 5-7) to the operation of the sterile reactor results in the characteristic exponential curve showing saturation of physical processes in the system within the first 3 days.

The accuracy of simulation of performance of media reactors depends on the accurate prediction of viable biomass in the reactor. Since the majority of the microbial species were unculturable using conventional methods, direct measurement of viable cell concentration was impossible. However, the activity of viable biomass in the reactors could be predicted based on the activity of known values from batch studies. In this study, the simulated performance of the microcosm reactors is plotted together with the simulated biomass activity as shown in Figures 5-10, 5-11 and 5-12 for the Reactors HR4, HR5 and HR7. Therefore the continuous flow systems provided an opportunity for the analysis of the biomass growth parameters and physical characteristics of the media.

The first system to be evaluated in detail was the reactor inoculated with live cultures from sludge but which was initially ridden of native soil biomass (Reactor HR4). The performance of this reactor shows the growth of Cr(VI) reducing species in the inoculum from sludge in the reactor devoid of other species could not be sustained in the absence of the native species. The simulation of Cr(VI) reduction shows initial removal probably from the delay in culture response as the Cr(VI) spread through the reactor. But after operation for 6.5 days, the toxicity in the reactor was probably too high for the culture. The culture started to die off in day 7 (Figure 5-10). In this simulation the biomass values of $X_{in} = 23.5 \text{ g/m}^3$, an X_{max} in the opposite direction =

3.5 g/m³, the logistic interval $t_0 = 10.4$ days, and pitch b of 5.03 were determined. The interstitial velocity u of 6.24×10^{-4} m/d was determined from measured values and the surface area in the reactor, a (L²), was estimated through parameter optimisation in AQUASIM. The model accurately predicted the trend of effluent Cr(VI) concentration in the reactor as shown by the dotted line against the effluent symbols in Figure 5-10.

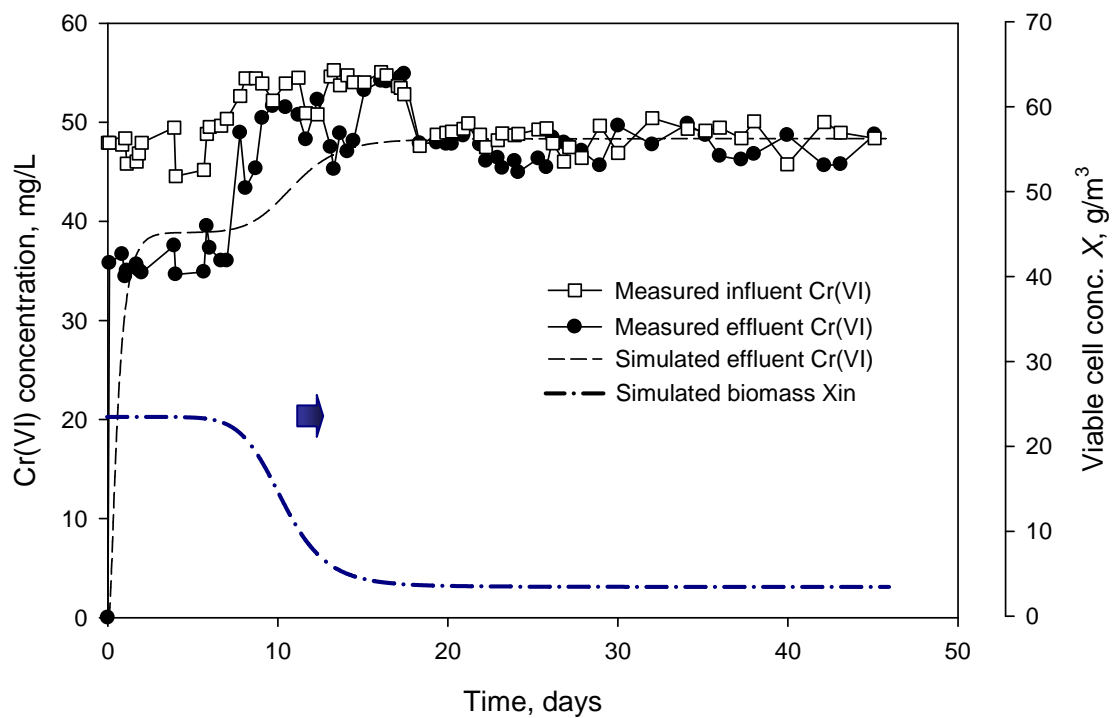


Figure 5-10: Model simulation of the sterilized microcosm reactor inoculated with live cultures from sludge (Reactor HR4).

5.5.3 Evaluation of the effect of carbon source using the model

In the second and third system, the performance of live cultures from both sources (soil and sludge) working together was evaluated. Reactor HR5 represents the operation on only inorganic carbon sources. Simulation of the system showed growth of biomass from a low inoculation value of approximately 8.5 g/m^3 to a maximum value of approximately 45.5 g/m^3 . The cell viability was reflected in the increased Cr(VI) reduction removal rate after 6 bed volumes (day 6). The characteristic flattening of the curve suggests an approach to the maximum cell growth and Cr(VI) reduction capacity of the reactor.

The best performance was observed in Reactor HR7 operated under carbon source. In this reactor, the simulated effluent continually increased with time and this was reflected in the ever increasing Cr(VI) reduction rate until the termination of the experiment at day 45. The continuing increase in the reduction rate is in agreement with the performance depicted by the cumulative Cr(VI) reduction (Figure 5-8). The trend in biomass from day 6 to 45 shows that the reactor supplied with carbon source had capacity for further Cr(VI) removal at the end of the experiment.

In this simulation, the system performed well regardless of having started with the lowest initial biomass value, $X_{in} = 4.5 \text{ g/m}^3$. The biomass in the reactor increased to approximately 65.5 g/m^3 a value more than 1.5 times higher than the maximum achievable cell concentration under no carbon source (Reactor HR5). The logistic time constant t_0 almost doubled to 10.4 days as X continued to increase. The pitch factor and interstitial velocity remained the same as under the other simulations conditions at 5.03 and $6.24 \times 10^{-4} \text{ m/d}$, respectively. The model simulation results helped validate the parameters previously determined in batch and made possible the

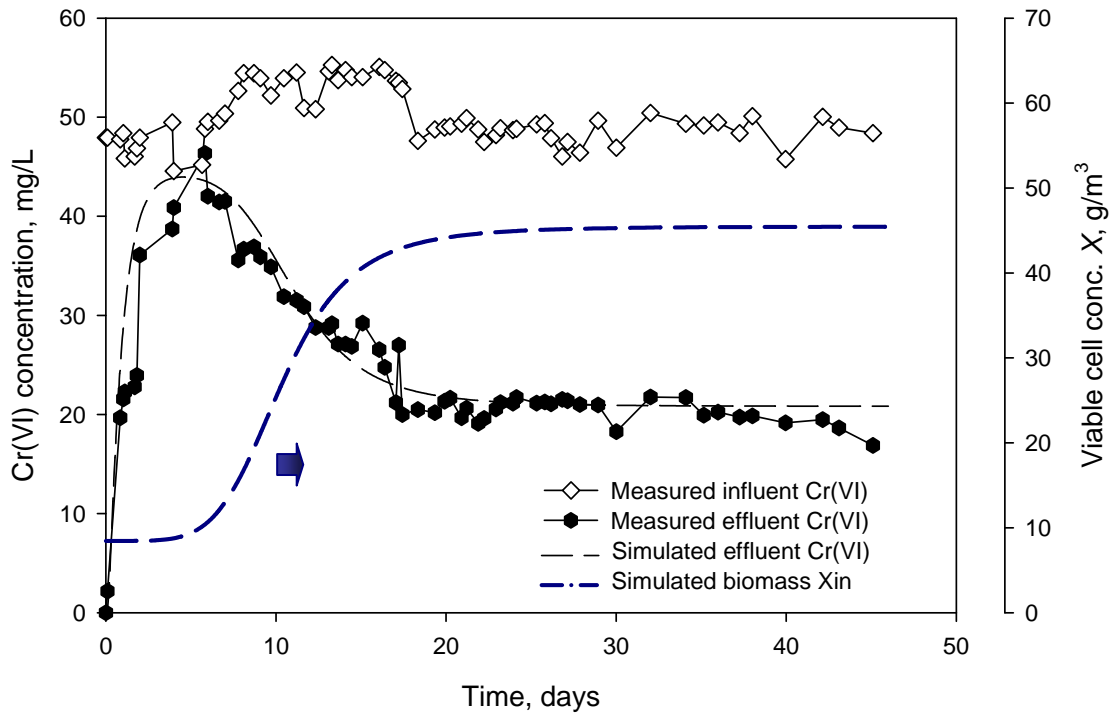


Figure 5-11: Model simulation of the live soil culture microcosm inoculated with live cultures from sludge and operated without carbon source (Reactor HR5).

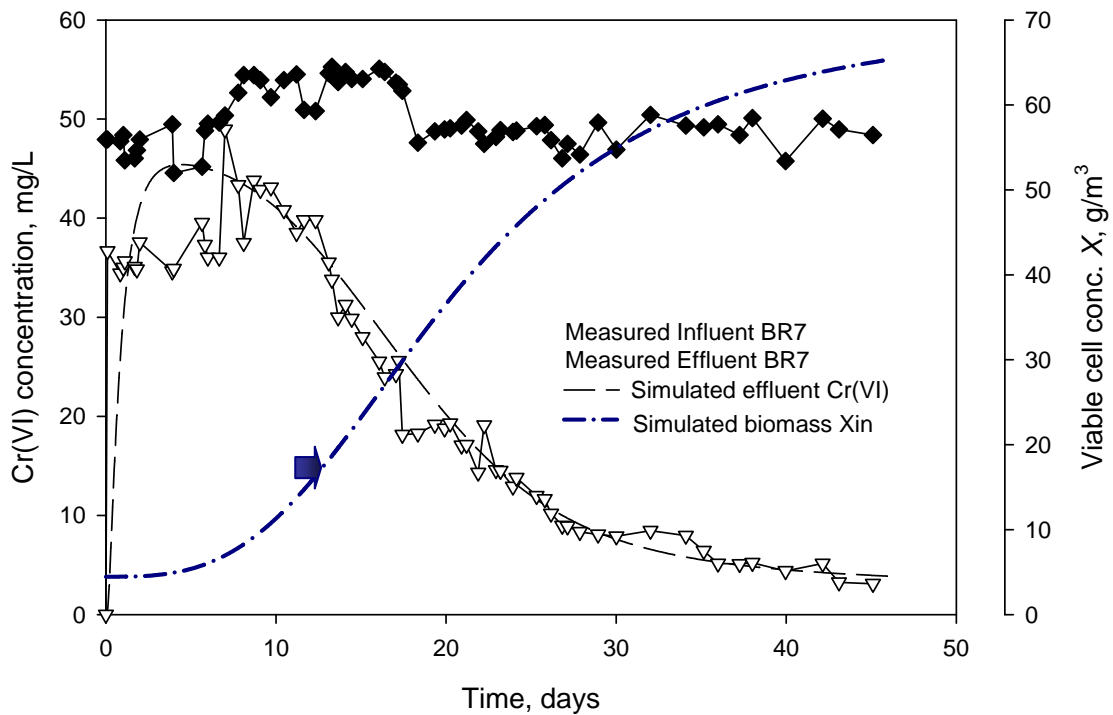


Figure 5-12: Model simulation of the live soil culture microcosm inoculated with live cultures from sludge and operated with carbon source (Reactor HR7).

evaluation of the viable biomass component which is difficult to measure directly in a heterogeneous media environment. All parameters used in the simulation of the microcosm reactor operation are summarised in Table 5-6.

Table 5-6: Final parameter values from the application and optimisation in the microcosm reactors.

Parameters Symbols	Associated Process	Optimum Value	Units
k_{mc}	Cr(VI) reduction rate	1.385	1/d
K_c	Cr(VI) reduction rate	2.450	mg/L
R_c	Cr(VI) reduction rate	0.533	mg/mg
K	Cr(VI) reduction rate	0.50	mg/L
C_r	Cr(VI) reduction rate	99	mg/L
b	Cell growth	3.0-8.0	--
t_o	Cell growth	10.4-20.4	d
X_0	Cell growth	4.5-23.5 (HR7-HR4)	g/m ³
X_{max}	Cell growth	3.5-65.3 (HR4-HR7)	g/m ³
C_s	Surface adsorption	1x10 ⁶	mg/kg
C_{crit}	Surface adsorption	0.01	mg/m ³
C_{smax}	Surface adsorption	0.00029	mg/kg
$alpha$	Surface adsorption ^a	0.5	--
$theta$	Surface adsorption ^a	0.4	--
rho_s	Surface adsorption ^a	2300	kg/m ³
C_{in}	Cr(VI) loading	50	mg/L
Q_{in}	Cr(VI) loading	0.001	m ³ /h
D	Column properties	98.4	m ² /h
A	Column properties	3.65-4.65 × 10 ⁻⁴	m ²
a	Column properties	variable	m ²

^a Stoichiometric coefficient for surface adsorption

5.6 Summary of Parameters

The model for the saturated soil column with dispersion which was adopted from AQUASIM 2.0 for the simulation of soil columns successfully simulated the operation of the microcosms used in this study. The breakthrough characteristics of the columns are typical of packed-media reactors with moderate dispersion depicting an exponential rise to a maximum followed by reduction in effluent as the Cr(VI) culture becomes more established.

The parameters for reaction rate processes were optimised in batch and were applied directly into the continuous flow process. Minor adjustments were applied to inhibition parameters due to the low levels of biomass in the continuous flow reactor systems compared to the batch systems. Different biomass values simulated in the reactor systems were attributed to different culture adaptability to high Cr(VI) loading. The culture grown under a carbon source showed a higher Cr(VI) reduction capacity than the cultures grown on organic sources from the soil.

Although, the model tracked successfully the trend in effluent Cr(VI) concentration in all the reactors tested, modifications would be required to take into consideration the loss of working volume and decreasing flow rate due to the growth of biomass in the reactors. The increase in biomass limits the working volume with time.

Some of the biomass related coefficients (i.e., X_o , X_{max} and t_0) converged at different values during optimisation since the biomass in the reactor varies as a function of available carbon source. Physical and chemical parameters were assumed constant within the applied experimental period.

5.7 Chapter Summary

Cr(VI) reduction capability was evaluated in this study in vadose reactors (VR) and unconfined aquifer reactors (HR) to simulate the behaviour of the pollutant and microcosms in aquifers. Results in vadose reactors showed the capability of Cr(VI) reducing species to reduce Cr(VI) and prevent the migration of Cr species across an inoculated barrier. The Cr(VI) reduction in the vadose reactors was achieved without any added carbon sources. The success of the inoculated reactors was mainly because the culture reconfigured into an optimal adapted culture for the reactor environment. This was demonstrated by analysing microbial culture composition in the reactor using 16S rRNA fingerprinting of the conserved 16S rRNA gene sequence.

The impact of a carbon source on Cr(VI) reduction and removal in an aquifer was evaluated using the HR system. It is expected that the water in the deep aquifer environment may be extremely low in organic carbon sources. The presence of an organic carbon source greatly enhanced the performance of the reactor. This was demonstrated by the high performance in reactors HR7 and HR8 which achieved up to 93% removal while operating in an oxygen deprived environment. Reactor HR5 and HR6 without carbon source achieved only about $66\pm 2\%$ and $73\pm 2\%$ removal, respectively. The reactor with native bacteria showed no chromium removal as an indication that the sludge bacteria were actively responsible for the reduction of chromium.

An advection-reaction model was used to successfully simulate effluent conditions. Reaction rate kinetic parameters optimised using batch data were used directly into the continuous flow reactor simulation. Most of the Physical-chemical parameters, apart from the media surface area a (L^2), were determined from known literature

values from similar systems. Only the mass transport parameters and adsorption parameters were estimated from the continuous flow reactor data.

CHAPTER 6

MESOCOSM STUDIES (BARRIER PERFORMANCE)

6.1 Background

This chapter reports on the performance prediction for a reactive barrier based on results from a laboratory mesocosm using aquifer media from a Cr(VI) contaminated site in South Africa. The mesocosm study was the second step towards the possible development of an *in situ* bioremediation process for field testing at a target contaminated site. The culture used in the mesocosm study was the same dried sludge culture tested in batch systems (Chapter 4) and in microcosm reactors (Chapter 5). The culture was originally isolated from sand drying beds from the Brits Wastewater Treatment Plant (Brits, North West Province). The mesocosm reactor was operated without any bioaugmentation – i.e., no additional nutrients or external carbon sources were introduced.

6.2 Simulation of Reactive Barrier: Mesocosm Reactor

An open top tank of (in cm) $123 \times 52 \times 50$ (L×B×H) was constructed from Plexiglas[®] (Evonik Röhm GmbH, Essen, Germany) reinforced by steel bars as shown earlier in Chapter 3 (Figure 3-4). The reactor was filled with aquifer medium compacted by hand to a compaction consistent with the ground conditions. Fourteen sample ports of 11 mm diameter glass tubing were inserted during placement of the aquifer material. Sample ports were strategically placed to capture the longitudinal and vertical concentration profiles and the concentration drop across the 19 cm wide microbial barrier (about the size of microcosm columns). Monitoring was conducted in the vertical direction at two depths of mesocosm: the deeper zone was monitored using

ports L1 to L7 and the shallower (medium) zone was monitored using the ports M1 to M7. Sampling the horizontal direction was conducted at positions 1 to 7 (P1 to P7). The data is presented two dimensions longitudinal (P1 to P7) and vertical (M and L)

6.3 Barrier Performance Evaluation (Qualitative)

From the 50th day the reactor started showing some yellow precipitate on top, this precipitate was observed on the whole top surface of the mesocosm reactor except the 19 cm biological permeable reactive barrier. The liquid which remained inside the mesocosm reactor turned greenish from the original hexavalent chromium yellowish colour. Studies done by Prat and colleagues (1997) for the reduction and precipitation of chromium using zero valent iron, have shown through X-ray Photoelectron Spectroscopy (XPS), that the chromium found within the precipitate is exclusively in the Cr(III) oxidation state, and that Fe present in the precipitate is in the Fe(III) oxidation state (Pratt et al., 1997). The AA was used to determine total chromium and an average of 90% of the chromium could be accounted for at the end of the experiment. This indicated that less than 10% may be adsorbed or retained onto soil particles during the cause of the experiment.

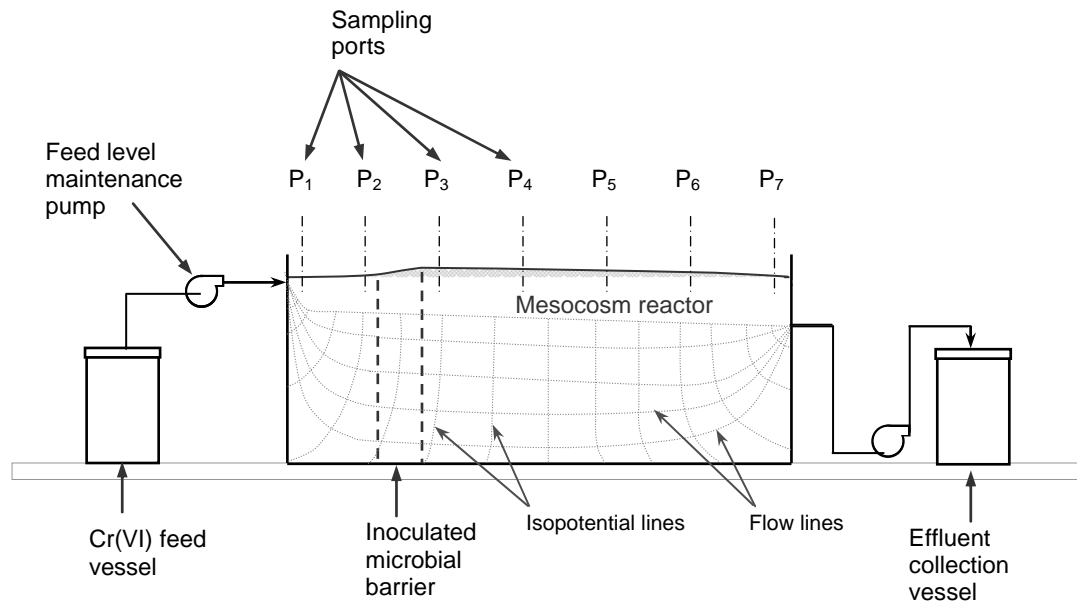


Figure 6-1: Schematic Representation of Mesocosm Reactor setup.

6.4 Barrier Performance Evaluation (Quantitative)

The results indicated that all the zones before the reactive barrier Zones 1M, 1L, 2M, 2L experienced no chromium reduction whereas most of the other zones after the reactive barrier experienced near total reduction after operation for more than 60 days. The set up of the ports in the reactor was in the following order; Zone 1 being the zone just before the feed area, Zone 2 the one just before the barrier, Zone 3 the zone just after the barrier followed by Zones 5 and 6 and finally Zone 7 the furthest away from the barrier but closer to the waste outlet. Figure 6-2 shows the reduction of chromium (VI) at different zones at level M (mid-depth of the reactor tank). The graph shows that there was visible reduction observed before the end of the first 30 days.

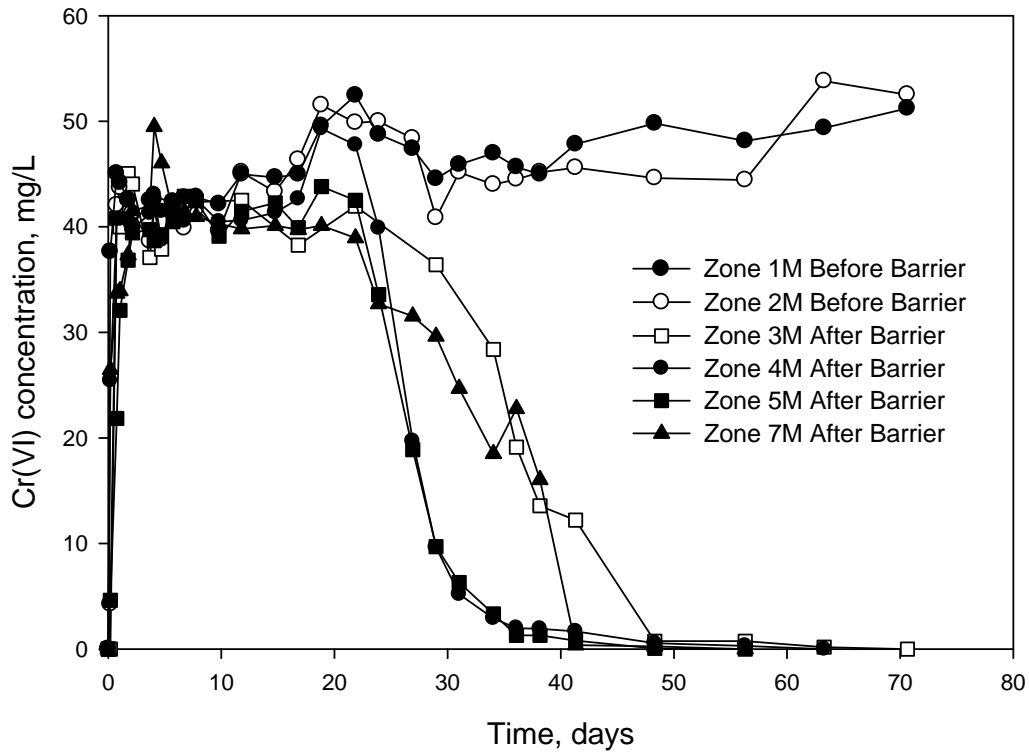


Figure 6-2: An overview of the reduction at level M (mid-depth of reactor).

In Figure 6-3, Zones 3L, 4L and 6L showed evidence of reduction after operation for approximately 21 days. Zone 4L and 6L reached near complete Cr(VI) removal before most of the zones at Level L. Samples from Zone 6L and 5L were the slowest performing of all zones. This could be a result of short circuiting or could have been caused by the presence of rocky material in the zone that interfered with flow nets in the vicinity. The problem of irregular flow resulted in slower dilution of the deeper zones during operation. This could be remedied by having a longer reactor to avoid rising flow lines towards the effluent ports which were at a height of approximately 25 cm from the bottom of the reactor. For the Level L, only the ports immediately after the barrier 3L and 4L reached 100% after day 40. This is because of more efficient dilution with the clean water coming through the microbial barrier. If the reactor operated under laminar flow conditions, the flow lines will be deepest in the region of Ports 3 and 4.

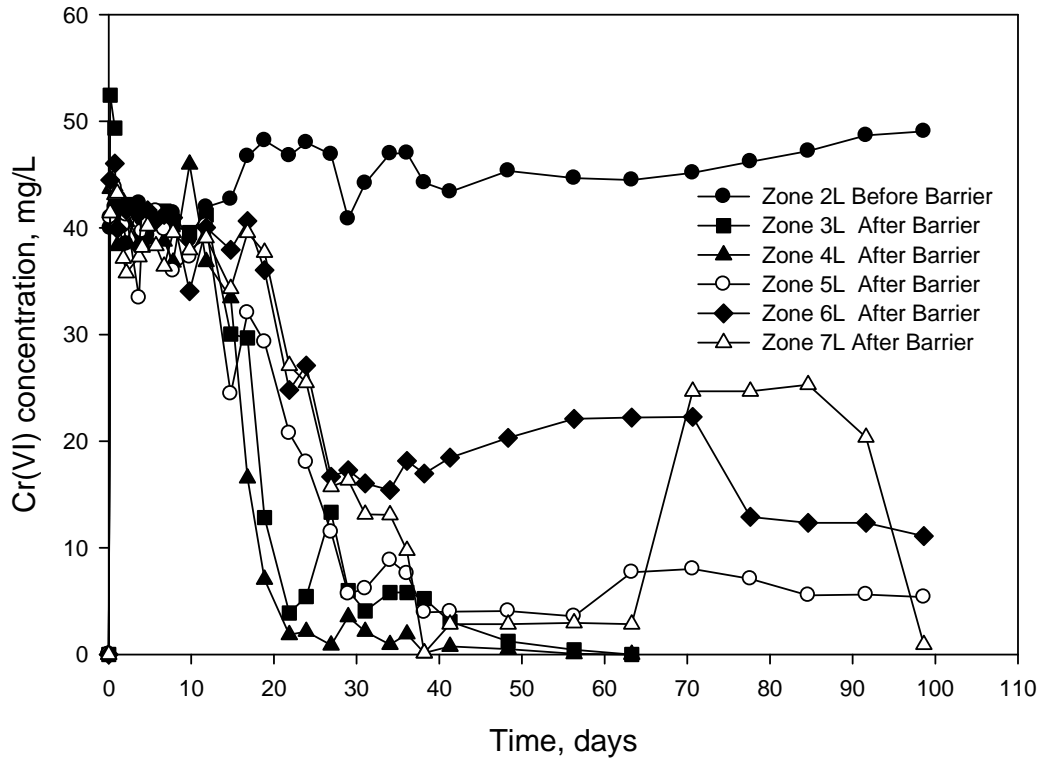


Figure 6-3: Barrier performance at level L (level near the bottom of the reactor).

The performance of the mesocosm reactor as monitored by bulk liquid concentration in samples drawn at the various ports is summarised in Table 6-1. The summary in this table clearly shows complete removal in barriers immediately after the barrier and some residual Cr(VI) concentration in the deeper zones of Ports 5 to 7.

Table 6-1: Summary of chromium (VI) reduction performance in the mesocosm reactor.

Zones	Remaining Cr(VI) Concentration After 13 Weeks ± 2 (mg/L)	Cr Removal %
2M(Pre barrier)	50	0
3M(Post barrier)	0	100
5M(Post barrier)	0	100
6M(Post barrier)	1.42	97
2L(Pre barrier)	49.5	5
3L(Post barrier)	0	0
5L(Post barrier)	5.3682	89
7L(Post barrier)	0.925	98

6.5 Spatial Variation at Discrete Time

The spatial Cr(VI) concentration profiles (snap shot profiles) in the mesocosm were calculated for specific time points – day 9.8, 26.9, 36.1, 48.3, and 63.3 as shown in Figure 6-4 for the mid-depth zone (M). Figure 6-4 illustrated the rate of Cr(VI) reduction in each specific port as time elapsed. It is clearly shown through Ports 3-7 that Cr(VI) was indeed continuously removed in the barrier and the rest of the ports (Ports 3-7) were cleaned up with time by dilution. It is also indicated that Port 7 was the slowest to clean probably due to rising flow lines at the end of the reactor which left a dead zone below Port 7.

Similar results were obtained in the deeper zone sampled by the long tubes (L). The samples for the Level L were analysed for a longer period – day 9.8, 26.9, 36.1, 48.3, 63.3, 84.6 and 98.6. Results from Figure 6-5 show that Ports 3 and 4 were cleaned up fast, receiving clean water from the barrier. The Ports downstream of Port 4 were the hardest to clean for the same reason as stated for Level M (above), that the flow lines were deepest in the region of Ports 3 and 4. It can therefore be concluded that, the closer the port to the barrier, the quicker the chromium is cleaned from the zone.

In spite of the difficulty of cleaning up 6L and 7L, it was demonstrated that these ports could be cleaned eventually as indicated by the low concentrations at day 98.6. At this point, Cr(VI) in zones 3 and 4 was completely removed.

The foregoing evaluation shows a two dimensional view of the spatial variability of Cr(VI) concentration in discrete time. This shows that studies at the mesocosm level will yield better representation of the three dimensional space and that spatial distribution parameters such as dispersion coefficient (D, L^2T^{-1}) and flow pattern as described by the Reynolds number could be important.

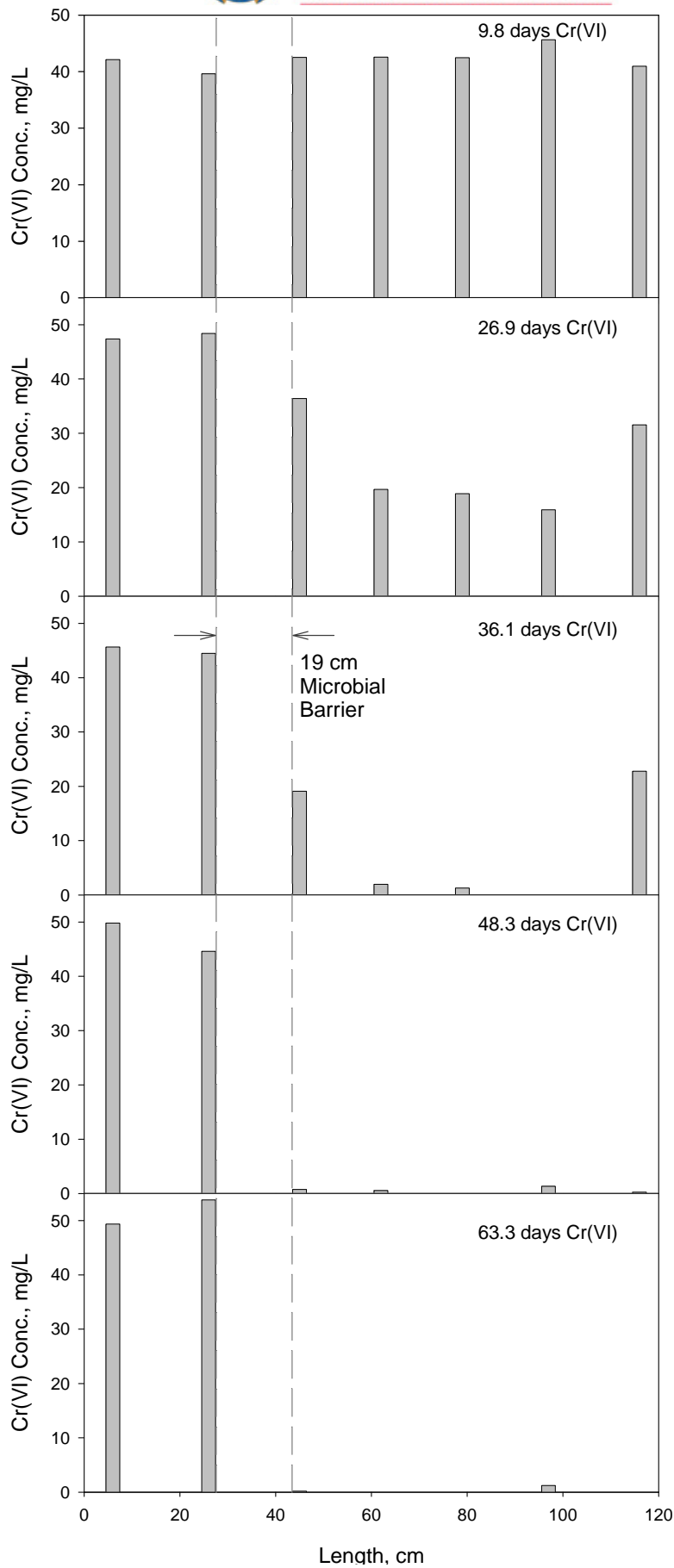


Figure 6-4: Cr(VI) reduction along the length of the mesocosm reactor at specific times showing the improving performance with time(Level M).

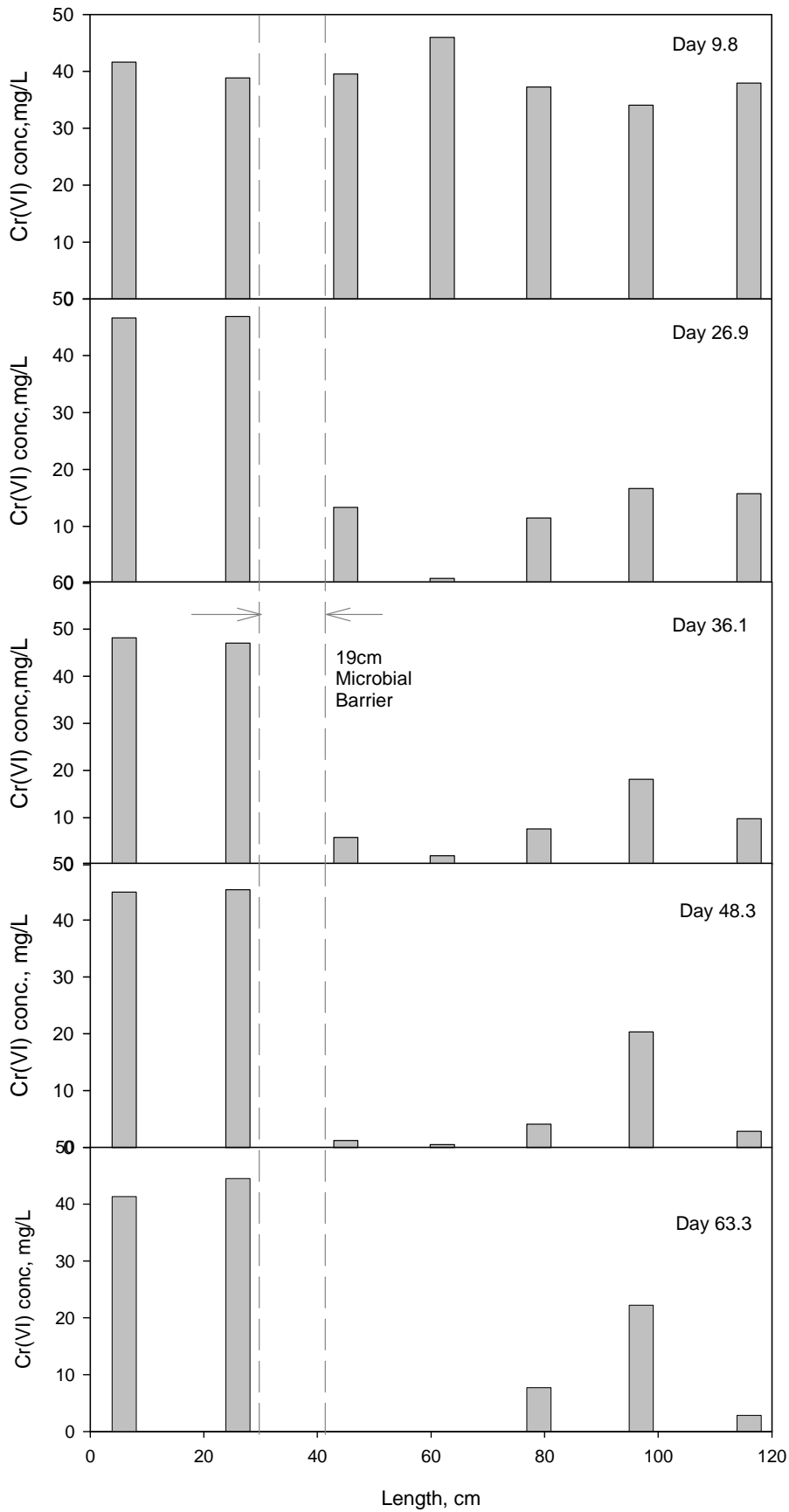


Figure 6-5: Cr(VI) reduction along the length of the mesocosm reactor at specific times showing the improving performance with time(Level L). (Continues/..).

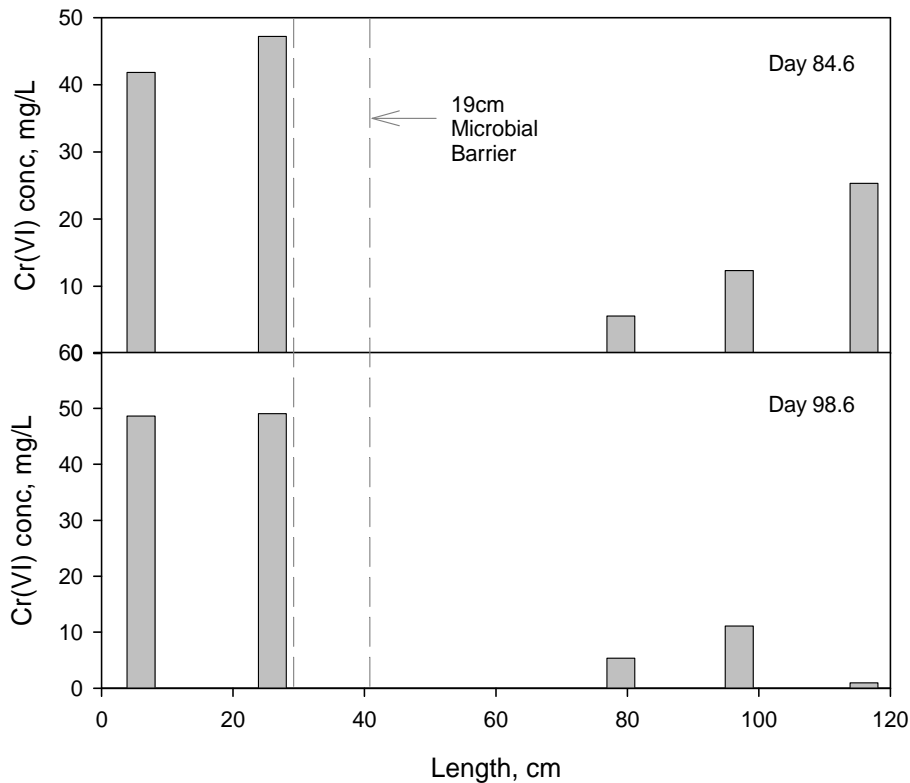


Figure 6-5: Cr(VI) reduction along the length of the mesocosm reactor at specific times showing the improving performance with time(Level L) (.../continued).

The cumulative reduction analysis was also assessed in the mesocosm studies in order to establish whether the microorganisms had reached their maximum performance ability. Figures 6-6 and 6-7 show that the reactor had not reached system failure yet for the larger part of the mesocosm reactor.

In Figures 6-6 and 6-7, zones 1M and 1 L were used as controls, respectively, since they were placed before the barrier presumably no Cr(VI) reduction was observed in these zones. The same scenario applied for the ports/zones 2M and 2L which showed minimal/zero chromium reduction. Based on the cumulative Cr(VI) reduction plot in Figures 6-6 and 6-7, the section of the reactor remained around the zero level in terms of culture capability since there was mostly no bacterial activity hence there was no Cr(VI) reduction.

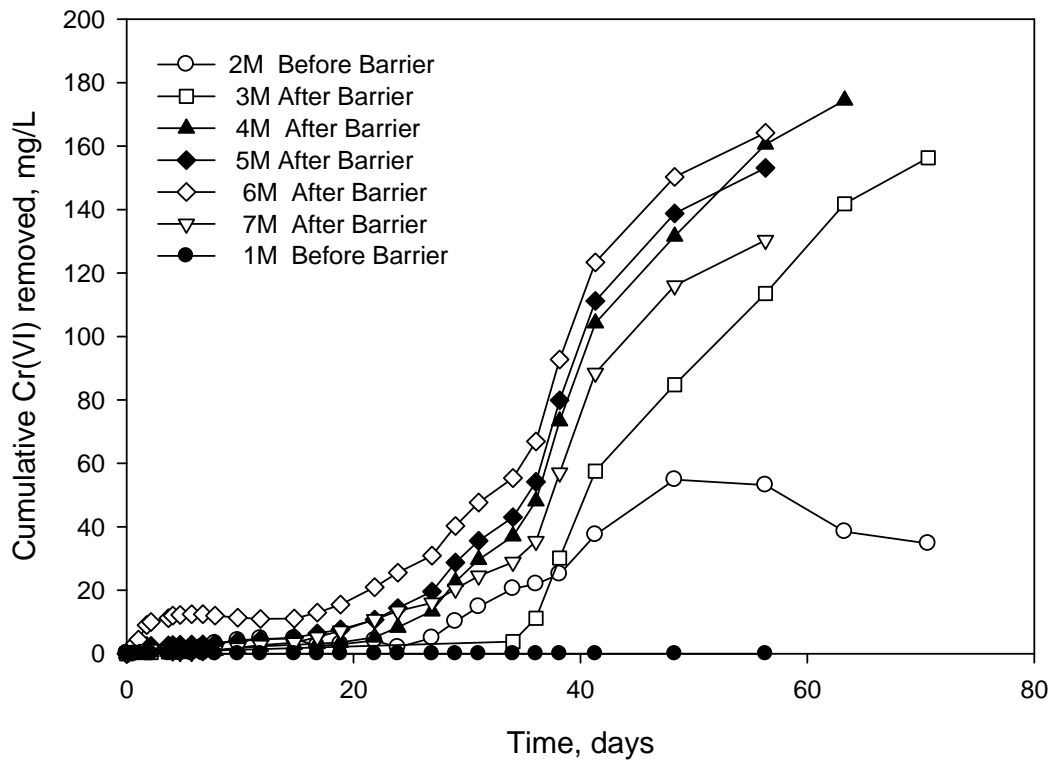


Figure 6-6: Cumulative Cr(VI) removal determined through concentration measurements in M-Zones.

Zone 2M showed a slight increase in performance from around day 29 of the experiment. The assumption is that microorganisms had started migrating towards the 2 zones therefore beginning to reduce chromium. The microbial activity then started to slow down after some time but there was still some activity until the experiment was terminated.

Similar analysis was conducted for the deep zones of the mesocosm reactor using samples collected from Level L. Ports 1L and 2L reflected near zero cumulative Cr(VI) removal suggesting no bacterial activity during the course of the experiment in the zone before the barrier, whereas all the samples after the barrier showed cumulative removal (Figure 6-7).

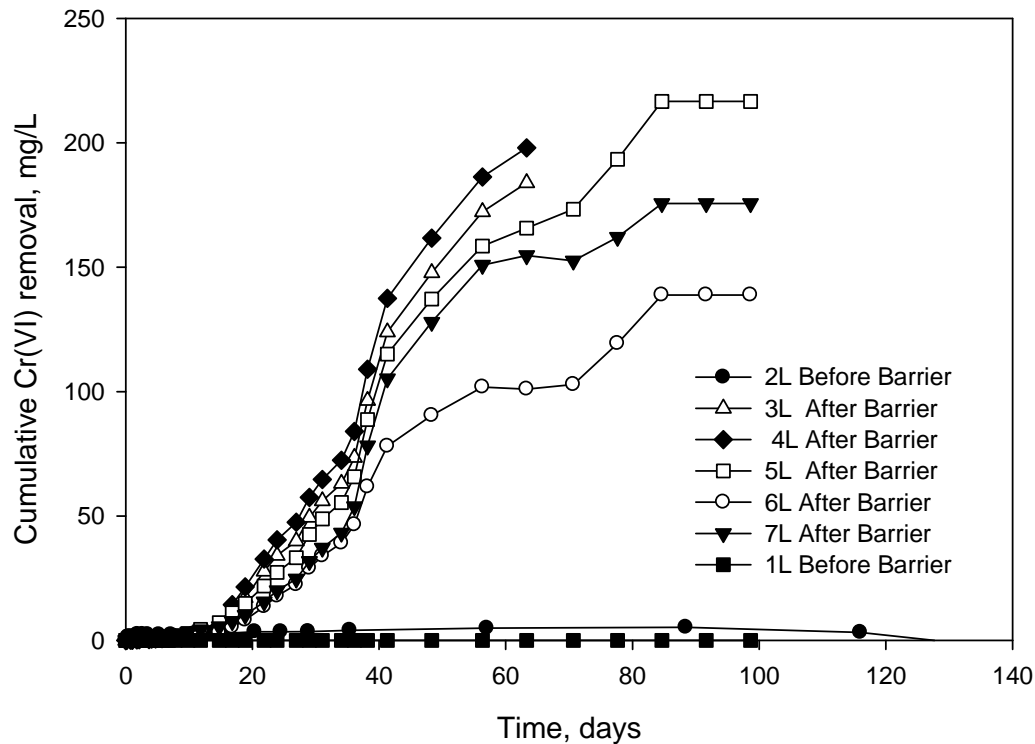


Figure 6-7: Cumulative Cr(VI) removal determined through concentration measurements in L-Zones.

6.6 Chapter Summary

The results from this study successfully demonstrated the ability of a permeable reactive microbial barrier to curb the spread of Cr(VI) pollution. This further highlights the potential of Cr(VI) reducing bacteria from activated sludge to both attenuate the spread of Cr(VI) pollution and the reduction of Cr(VI) in aquifer material. This could be a good starting point in the formulation of a pilot study on biological permeable barriers for protection against the spread of the Cr(VI) contaminant from hot spots in the area. Figure 6-8 shows a proposed barrier concept around the hotspots.

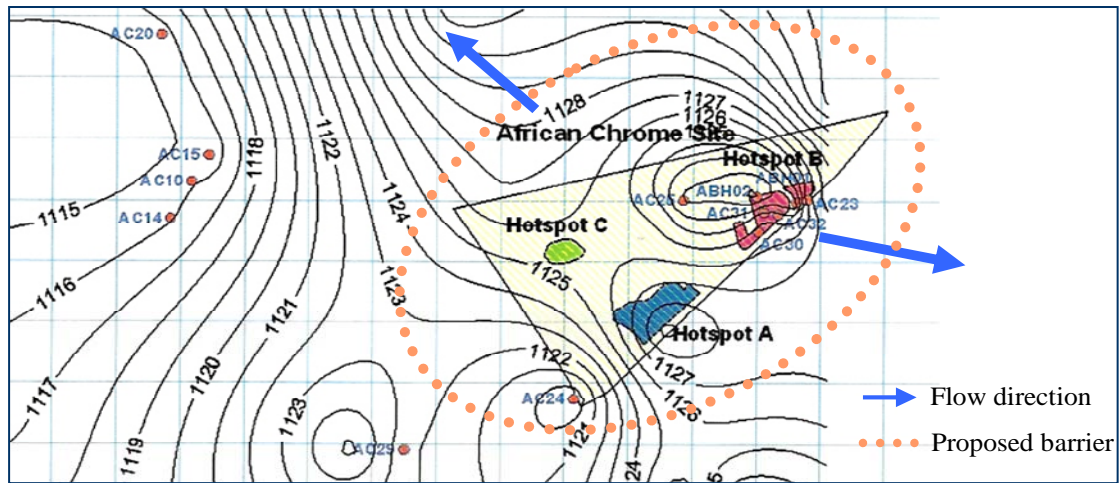


Figure 6-8: Proposed strategic positioning of the biological permeable reactive barrier at the target bioremediation site in Brits.

The cumulative results showed that the microbial activity in the mesocosm reactor system was still high at the time the experiment was terminated, which means the microorganisms could still be able to reduce hexavalent chromium at a higher loading than applied in this study. This on its own is a positive milestone since the annual average concentration at the proposed distance to the barrier at the target site has been reported to be approximately 40 mg/L, 20% lower than the applied 50 mg/L in this study.

CHAPTER 7

SUMMARY AND CONCLUSIONS

Batch experiments under varying initial Cr(VI) concentration of 50-400 mg/L in media with harvested and concentrated cells showed that the indigenous culture achieved complete Cr(VI) removal under initial concentration up to 200 mg/L in less than 64.3 hours (2.7 days). Up to 94% of Cr(VI) was removed at the initial concentration of 300 mg/L after incubation for 110 hours whereas tests under anaerobic conditions were conducted over a lower concentration range of 50 mg/L to 300 mg/L. The rate of Cr(VI) reduction was generally slower in the anaerobic cultures. Near total Cr(VI) reduction occurred in cultures with a lower initial Cr(VI) concentration of 150 mg/L after a longer incubation period of 155 hours compared with aerobic cultures.

The feasibility of using Cr(VI) reducing microorganisms in vadoze zone material was demonstrated by better performance of microcosm reactors inoculated with a locally isolated consortium of Cr(VI) reducing organisms than sterilized controls. The inoculated reactor achieved near complete removal of Cr(VI) (95.3 %) while operating under a low hydraulic loading after 17 days at 40 mg/L. The inhibitory effect of Cr(VI) on the Cr(VI) reducing microorganisms was demonstrated by the decrease in Cr(VI) reduction rate in reactor VR3 which operated at twice the hydraulic loading rate of reactor VR6.

Microcosm reactors with saw dust performed better than the ones with no carbon source, the best performing reactor after about 45 days of operation at 50 mg/L of chromium was 93%. Microbial culture conditions in the best performing microcosms from the microaerobic vadose zone favoured the Cr(VI) reducing species, *Bacillus*

cereus/thirungiensis and *Lysinibacillus sphaericus*, probably originating from the sludge. Microbial culture composition in anaerobic deep aquifer microcosms was predominated by anaerobic Gram-negative species.

The batch modelling results showed that the performance of the bacteria fitted best the non-competitive inhibition model with cell inactivation under aerobic conditions, whereas the competitive inhibition was effective above a threshold concentration of about 100 mg/L under anaerobic conditions. The model used for aquifer zone simulation (HR) was adopted from AQUASIM 2.0. The model simulated the operation of a soil column with dispersion and a plug flow regime. Most of the reaction rate kinetic parameters optimised using batch data were used directly in the continuous flow reactor simulation. Reaction rate kinetics predominated during operation without carbon source due to low biomass activity.

Experimental results from Mesocosm experiments showed that 50 mg/L of hexavalent chromium was completely reduced after operation for approximately 9 weeks as measured in the ports just after the barrier. The ports before the barrier showed no chromium reduction. The outcome of this study is a good basis for testing the concept in a pilot study on site.

The microbial reactive barrier has performed well in this study with significant reduction in all zones and an average of approximately 90% in the final effluent. The outcome of the mesocosm results could be useful in the formulation of biological permeable barriers for protection against the spread of the pollutant from hot spots in the area.